AOP ID and Title:

AOP 379: Increased susceptibility to viral entry and coronavirus production leading to thrombosis and disseminated intravascular coagulation
Short Title: SARS-CoV2 to thrombosis and DIC

Graphical Representation

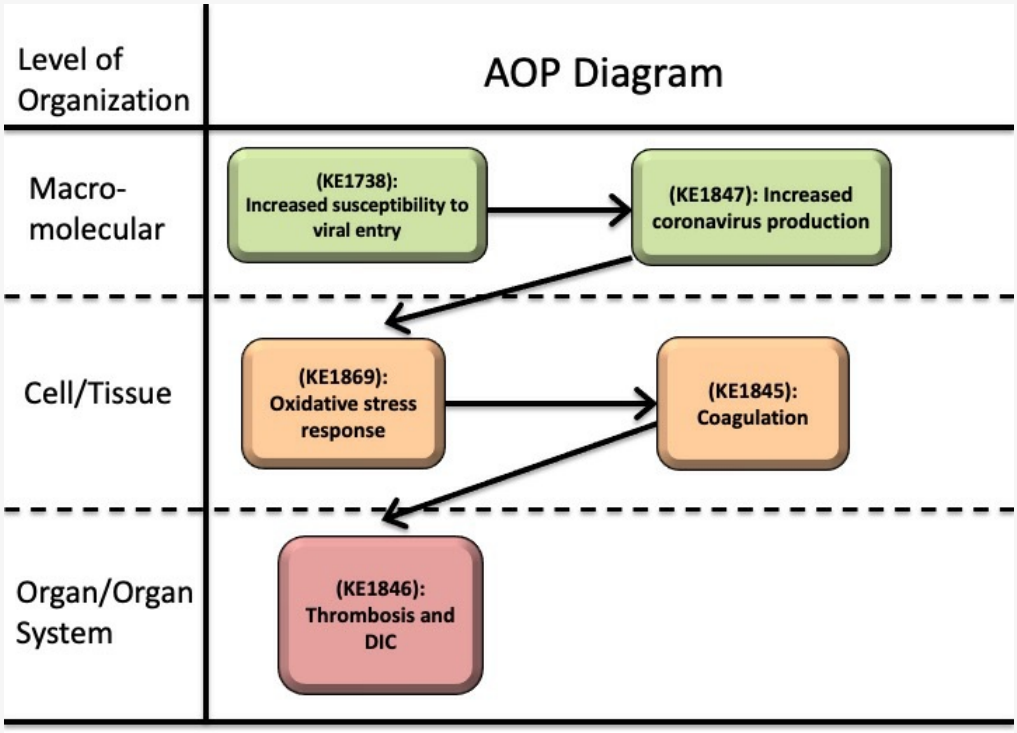

Authors

Shihori Tanabe, Young-J Kim, Alicia Paini, Sally Mayasich, Maria J Amorim, Alan Hargreaves, Penny Nymark, Marvin Martens, Dan Jacobson, Felicity Gavins, Luigi Margiotta-Casaluci, Sabina Halappanavar, Natalia Reyero, Julija Filipovska, Steve Edwards, Rebecca Ram, Adrienne Layton, and CIAO members

Status

Author status	OECD status	OECD project	SAAOP status
Under development: Not open for comment. Do not cite			

Abstract

Coronavirus disease-19 (COVID-19) is circulating all over the world. To understand and find a way of the COVID-19 treatment, the therapeutic mechanism of COVID-19 is focused on in this Editorial. The pathogenesis of COVID-19 includes molecular networks such as the binding of the membrane proteins, signaling pathways, and RNA replication. The mechanism of infection and targets of the therapeutics are explored and summarized. The severe acute respiratory syndrome coronavirus 2 (SARS-CoV-2), which is a new type of coronavirus causing COVID-19, infects the cells via the binding of the membrane proteins of human cells and is internalized by the cells. The viral genome is replicated by RNA-dependent RNA polymerase (RdRp), followed by the packaging and releasing of the viral particles. These steps can be the main targets for the therapeutics of COVID-19. This AOP379 "Increased susceptibility to viral entry and coronavirus production leading to thrombosis and disseminated intravascular coagulation" consists of the molecular initiating events (MIE) as "Increased susceptibility to viral entry" (KE1738) and "Increased coronavirus production" (KE1847), key events (KEs) as "Oxidative stress response" (KE1869) and "Coagulation" (KE1845), and adverse outcome (AO) as "Thrombosis and Disseminated Intravascular Coagulation" (KE1846).

Summary of the AOP

Events

Molecular Initiating Events (MIE), Key Events (KE), Adverse Outcomes (AO)

Sequence	Type	Event ID	Title	Short name
1	MIE	1738	Increased susceptibility to viral entry	Increased susceptibility to viral entry
2	MIE	1847	Increased coronavirus production	Increased SARS-CoV-2 production
3	KE	1869	Oxidative stress response	Response to ROS
4	KE	1845	Coagulation	Coagulation
5	AO	1846	Thrombosis and Disseminated Intravascular Coagulation	Thrombosis and DIC

Key Event Relationships

Upstream Event	Relationship Type	Downstream Event	Evidence	Quantitative Understanding
Increased susceptibility to viral entry	adjacent	Increased coronavirus production	High	Moderate
Increased coronavirus production	adjacent	Oxidative stress response	Moderate	Not Specified
Oxidative stress response	adjacent	Coagulation	Moderate	Not Specified
Coagulation	adjacent	Oxidative stress response	Moderate	Not Specified
Coagulation	adjacent	Thrombosis and Disseminated Intravascular Coagulation	High	

Stressors

Name	Evidence
Stressor:624 SARS-CoV-2	High

Overall Assessment of the AOP

Domain of Applicability

Life Stage Applicability

Life Stage	Evidence
All life stages	Moderate

Taxonomic Applicability

Term	Scientific Term	Evidence	Links
Homo sapiens	Homo sapiens	High	NCBI

Sex Applicability

Sex	Evidence
Unspecific	High

References

1. Cui J, Li F, Shi ZL. Origin and evolution of pathogenic Coronaviruses. Nature Reviews Microbiology. 2019;17(3):181-192.

2. Chen B, Tian EK, He B, Tian L, Han R, Wang S, et al. Overview of lethal human Coronaviruses. Signal Transduction and Targeted Therapy, 2020;5(1):89.

3. Florindo HF, Kleiner R, Vaskovich-Koubi D, Acúrcio RC, Carreira B, Yeini,E, et al. Immune-mediated approaches against COVID-19. Nature Nanotechnology. 2020:15(8):630-45.

4. Blanco Melo D, Nilsson-Payant BE, Liu WC, Uhl S, Hoagland D, Møller R, et al. Imbalanced Host Response to SARS-CoV-2 Drives Development of COVID-19. Cell. 181;(5):1036-1045.

5. Pizzorno A, Padey B, Julien T, Trouillet-Assant S, Traversier A, Errazuriz-Cerda E, et al. Characterization and Treatment of SARS-CoV-2 in Nasal and Bronchial Human Airway Epithelia. Cell Reports Medicine. 2020:1(4).

6. Riva L, Yuan S, Yin X, Martin-Sancho L, Matsunaga N, Pache L, et al. Discovery of SARS-CoV-2 antiviral drugs through large-scale compound repurposing. Nature. 2020.

7. Kowalewski J, Ray A. Predicting novel drugs for SARS-CoV-2 using machine learning from a & g 10 million chemical space. Heliyon. 2020;6(8).

6. Tanabe S. The Therapeutic Mechanism of COVID-19. J Clin Med Res. 2020;2(5):1-3. DOI: https://doi.org/10.37191/Mapsci-2582-4333-2(5)-048

Appendix 1

List of MIEs in this AOP

Event: 1738: Increased susceptibility to viral entry

Short Name: Increased susceptibility to viral entry

AOPs Including This Key Event

AOP ID and Name	Event Type
Aop:320 - Binding of viral S-glycoprotein to ACE2 receptor leading to acute respiratory distress associated mortality	KeyEvent
Aop:379 - Increased susceptibility to viral entry and coronavirus production leading to thrombosis and disseminated intravascular coagulation	MolecularInitiatingEvent

Stressors

Name
Sars-CoV-2

Biological Context

Level of Biological Organization

Molecular

Cell term

Cell term

cell

Organ term

Organ term

organ

Domain of Applicability

Taxonomic Applicability

Term	Scientific Term	Evidence	Links
Homo sapiens	Homo sapiens	High	NCBI

Life Stage Applicability

Life Stage	Evidence
All life stages	High

Sex Applicability

Sex	Evidence
Unspecific	High

Homo sapiens

ACE 2 is highly expressed in gastrointestinal system such as small intestine and duodenum, as well as oral and nasal mucosa, lung, kidney and brain [6-8].

Key Event Description

Coronavirus, which is a nanoparticle, is sphere-shaped and its diameter is 80-120 nm on average, where it sometimes ranges from 50 nm to 200 nm [Masters PS. (2006)]. Spike protein (S protein), the so-called peplomer, on the surface of the particle binds to the receptor on the host cellular membrane, then internalized inside the cells. Viral RNA (plus strand) in the viral particles is replicated and translated into the viral structural protein in the host cells, which is followed by replication of new viral particles [Weiss SR, Navas-Martin S. (2005)]. Coronavirus is recognized by the binding of S protein on the viral surface and angiotensin I converting enzyme 2 (ACE2) receptor on the cellular membrane, then internalized into the cell via processing of S protein by transmembrane serine protease 2 (TMPRSS2) protease [Hoffmann M, et al. (2020)]. The inhibition of this internalization of the viral particle would theoretically prevent the viral infection and replication [Tanabe S. (2020)].

How it is Measured or Detected

SARS-CoV entry can be determined by quantitative RT-PCR specific to the subgenomic mRNA of the N transcript, following the infection of the 293T-hACE2 cells with SARS-CoV [Glowacka I, et al. (2011)].

For analyzing cell entry of S protein of SARS-CoV-2, vesicular stomatitis virus (VSV) particles expressing eGFP and firefly luciferase bearing SARS-2-S are cultured with cell lines, followed by determining luciferase activity in cell lysates [Hoffmann M, et al. (2020)].

References

1. Masters PS. (2006) The molecular biology of coronaviruses. Adv Virus Res. 66:193-292.
2. Weiss SR, Navas-Martin S. (2005) Coronavirus pathogenesis and the emerging pathogen severe acute respiratory syndrome coronavirus. Microbiol Mol Biol Rev. 69(4):635-64.
3. Hoffmann M, Kleine-Weber H, Schroeder S, Krüger N, Herrler T, et al. (2020).SARS-CoV-2 Cell Entry

Depends on ACE2 and TMPRSS2 and Is Blocked by a Clinically Proven Protease Inhibitor. Cell. 181(2):271-280.e278.

4. Tanabe S. (2020) Cellular Internalization and RNA Regulation of RNA Virus. Adv Clin Med Res. 1(1):1-3.
5. Glowacka I, Bertram S, Müller MA, Allen P, Soilleux E, Pfefferle S, et al. Evidence that TMPRSS2 Activates the Severe Acute Respiratory Syndrome Coronavirus Spike Protein for Membrane Fusion and Reduces Viral Control by the Humoral Immune Response. Journal of Virology. 2011;85(9):4122.
6. Fagerberg L, Hallström BM, Oksvold P, Kampf C. Djureinovic D, et al. (2014) Analysis of the human tissue- specific expression by genome-wide integration of transcriptomics and antibody-based proteomics. Mol Cell Proteomics. 13(2):397-406.
7. Farmer D, Gilbert M, Borman R, Clark KL. (2002) Quantitative mRNA expression profiling of ACE 2, a novel homologue of angiotensin converting enzyme. FEBS Lett. 532(1-2):107-110.
8. Xu H, Zhong L, Deng J, Peng J, Dan H, et al. (2020) High expression of ACE2 receptor of 2019-nCoV on the epithelial cells of oral mucosa. Int J Oral Science. 12(1):8.

Event: 1847: Increased coronavirus production

Short Name: Increased SARS-CoV-2 production

Key Event Component

Process	Object	Action
viral RNA genome replication	viral RNA-directed RNA polymerase complex	increased
positive stranded viral RNA replication	viral RNA-directed RNA polymerase complex	increased
viral RNA genome packaging	viral assembly compartment	increased
mRNA transcription	ssRNA viral genome	increased
viral translation	ssRNA viral genome	increased

AOPs Including This Key Event

AOP ID and Name	Event Type
Aop:379 - Increased susceptibility to viral entry and coronavirus production leading to thrombosis and disseminated intravascular coagulation	MolecularInitiatingEvent
Aop:320 - Binding of viral S-glycoprotein to ACE2 receptor leading to acute respiratory distress associated mortality	KeyEvent

Stressors

Name
Sars-CoV-2

Biological Context

Level of Biological Organization

Cellular

Cell term

Cell term

cell

Organ term

Organ term

organ

Domain of Applicability

Taxonomic Applicability

Term	Scientific Term	Evidence	Links
Homo sapiens	Homo sapiens	High	NCBI
Mus musculus	Mus musculus	Moderate	NCBI
Mustela putorius furo	Mustela putorius furo	Moderate	NCBI

Life Stage Applicability

Life Stage	Evidence
All life stages	High

Sex Applicability

Sex	Evidence
Unspecific	High

Broad mammalian host range has been demonstrated based on spike protein tropism for and binding to ACE2 [Conceicao *et al.* 2020; Wu *et al.* 2020] and cross-species ACE2 structural analysis [Damas *et al.* 2020]. No literature has been found on primary translation and molecular interactions of nsps in non-human host cells, but it is assumed to occur if the virus replicates in other species.

Very broad mammalian tropism: human, bat, cat, dog, civet, ferret, horse, pig, sheep, goat, water buffalo, cattle, rabbit, hamster, mouse

Key Event Description

This KE1847 "Increase coronavirus production" deals with how the genome of the severe acute respiratory syndrome coronavirus 2 (SARS-CoV-2) is translated, replicated, and transcribed in detail, and how the genomic RNA (gRNA) is packaged, and the virions are assembled and released from the cell.

Coronavirus is a class of viruses that have single-stranded positive-sense RNA genomes in their envelopes [D. Kim *et al.*]. The virus contains a 29.7 kB positive-sense RNA genome flanked by 5' and 3' untranslated regions of 265 and 342 nucleotides, respectively [E. J. Snijder *et al.*] that contain cis-acting secondary RNA structures essential for RNA synthesis [N. C. Huston *et al.*]. The genome just prior to the 5′ end contains the transcriptional regulatory sequence leader (TRS-L) [C.J. Budzilowicx *et al.*]. The SARS-CoV genome is polycistronic and contains 14 open reading frames (ORFs) that are expressed by poorly understood mechanisms [E. J. Snijder *et al.*]. Preceding each ORF there are other TRSs called the body TRS (TRS B). The 5′ two-thirds of the genome contains two large, overlapping, nonstructural ORFs and the 3′ third contains the remainder ORFs [H. Di *et al.*]. Genome expression starts with the translation of two large ORFs of the 5' two-thirds: ORF1a of 4382 amino acids and ORF1ab of 7073 amino acid that occurs via a programmed (- 1) ribosomal frameshifting [E. J. Snider *et al.*], yielding pp1a and pp1ab. These two polyproteins are cleaved into 16 subunits by two viral proteinases encoded by ORF1a, nsp3, and nsp5 that contain a papain-like protease domain and a 3C-like protease domain [M. D. Sacco *et al.*]. The processing products are a group of replicative enzymes, named nsp1-nsp16, that assemble into a viral replication and transcription complex (RTC) associated with membranes of endoplasmic reticulum (ER) with the help of various membrane-associated viral proteins [S. Klein *et al.*, E. J. Snijder *et al.,* P. V'Kovski, *et al.*]. Besides replication, which yields the positive-sense gRNA, the replicase also mediates transcription leading to the synthesis of a nested set of subgenomic (sg) mRNAs to express all ORFs downstream of ORF1b that encode structural and accessory viral proteins. These localize to the 3′ one-third of the genome, as stated above, and result in a 3′ coterminal nested set of 7–9 mRNAs that share ~70–90 nucleotide (nt) in the 5′ leader and that is identical to the 5′ end of the genome [P. Liu, and J. Leibowitz]. sgRNAs encode conserved structural proteins (spike protein [S], envelope protein [E], membrane protein [M], and nucleocapsid protein [N]), and several accessory proteins. SARS-CoV-2 is known to have at least six accessory proteins (3a, 6, 7a, 7b, 8, and 10). Overall the virus is predicted to express 29 proteins [D. Kim *et al.*]. The gRNA is packaged by the structural proteins to assemble progeny virions.

Viral translation:

SARS-CoV-2 is an enveloped virus with a single-stranded RNA genome of ~30 kb, sequence orientation in a 5' to 3' direction typical of positive sense and reflective of the resulting mRNA [D. Kim *et al.*]. The SARS-CoV-2 genome contains a 5'-untranslated region (UTR; 265 bp), ORF1ab (21,289 bp) holding two overlapping open reading frames (13,217 bp and 21,289 bp, respectively) that encode two polyproteins [D. Kim *et al.*]. Other elements of the genome include are shown below [V. B. O'Leary *et al.*]. **The first event upon cell entry is the primary translation of the ORF1a and ORF1b gRNA to produce non-structural proteins (nsps).**

This is completely dependent on the translation machinery of the host cell. Due to fewer rare “slow-codons”, SARS-CoV-2 may have a higher protein translational rate, and therefore higher infectivity compared to other coronavirus groups [V. B. O'Leary *et al.*]. The ORF1a produces polypeptide 1a (pp1a, 440–500 kDa) that is cleaved into nsp-1 through nsp-11. A -1 ribosome frameshift occurs immediately upstream of the ORF1a stop codon, to allow translation through ORF1b, yielding 740–810 kDa polypeptide pp1ab, which is cleaved into 15 nsps [D. Kim *et al.*].

Two overlapping ORFs, ORF1a and ORF1b, generate continuous polypeptides, which are cleaved into a total of 16 so-called nsps [Y Finkel *et al.*]. Functionally, there are five proteins from pp1ab (nsp-12 through nsp-16) as nsp-1-11 are duplications of the proteins in pp1a due to the ORF overlap. The pp1a is approximately 1.4–2.2 times more expressed than pp1ab. After translation, the polyproteins are cleaved by viral proteases nsp3 and nsp5. Nsp5 protease can be referred to as 3C-like protease ($3CL^{pro}$) or as main protease (M^{pro}), as it cleaves the majority of the polyprotein cleavage sites. [H.A. Hussein *et al.*] Nsp1 cleavage is quick and nsp1 associates with host cell ribosomes and results in host cellular shutdown, suppressing host gene expression [M. Thoms *et al.].* Fifteen proteins, nsp2–16 constitute the viral RTC. They are targeted to defined subcellular locations and establish a network with host cell factors. Nsp2–11 remodel host membrane architecture, mediate host immune evasion and provide cofactors for replication, whilst nsp12–16 contain the core enzymatic functions involved in RNA synthesis, modification and proofreading [P. V'Kovski *et al.*]. nsp-7 and nsp-8 form a complex priming the RNA-dependent RNA polymerase (RdRp or RTC) - nsp-12. nsp14 provides a 3′–5′ exonuclease activity providing RNA proofreading function. Nsp-10 composes the RNA capping machinery nsp-9. nsp13 provides the RNA 5′-triphosphatase activity. Nsp-14 is a *N*7-methyltransferase and nsp-16 the 2′-*O*-methyltransferase. Many of the nsps have multiple functions and many viral proteins are involved in innate immunity inhibition. Nsp-3 is involved in vesicle formation along with nsp-4 and nsp-6 where viral replication occurs. Interactions between SARS-CoV-2 proteins and human RNAs thwart the IFN response upon infection: nsp-16 binds to U1 and U2 splicing RNAs to suppress global mRNA splicing; nsp-1 binds to 40S ribosomal RNA in the mRNA entry channel of the ribosome to inhibit host mRNA translation; nsp-8 and nsp-9 bind to the 7SL RNA to block protein trafficking to the cell membrane [A. K. Banerjee *et al.*]. Xia et al. [H. Xia *et al.*] found that nsp-6 and nsp-13 antagonize IFN-I production via distinct mechanisms: nsp-6 binds TANK binding kinase 1 (TBK1) to suppress interferon regulatory factor 3 (IRF3) phosphorylation, and nsp-13 binds and blocks TBK1 phosphorylation.

Viral transcription and replication:

Viral transcription and replication occur at the viral replication organelle (RO) [E. J. Snijder *et al.*]. The RO is specifically formed during infection by reshaping ER and other membranes, giving rise to small spherular invaginations, and large vesiculotubular clusters, consisting of single- and/or double-membrane vesicles (DMV), convoluted membranes (CM) and double-membrane spherules invaginating from the ER [S. Klein *et al.,* E. J. Snijder *et al.*]. There is some evidence that DMV accommodate viral replication which is based on radiolabelling viral RNA with nucleoside precursor ([5-^{3}[H]uridine) and detection by EM autoradiography [E. J. Snijder *et al.*].

Viral replicative proteins and specific host factors are recruited to ROs [E. J. Snijder *et al.*]. RNA viral genome is transcribed into messenger RNA by the viral RTC [P. Ahlquist *et al.*]. Viral RTC act in combination with other viral and host factors involved in selecting template RNAs, elongating RNA synthesis, differentiating genomic RNA replication from mRNA transcription, modifying product RNAs with 5' caps or 3' polyadenylate [P. Ahlquist *et al.*]. Positive-sense (messenger-sense) RNA viruses replicate their genomes through negative-strand RNA intermediates [M. Schwartz *et al.*]. The intermediates comprise full-length negative-sense complementary copies of the genome, which functions as templates for the generation of new positive-sense gRNA, and a nested set of sg mRNAs that lead to the expression of proteins encoded in all ORFs downstream of ORF1b. The transcription of coronaviruses is a discontinuous process that produces nested 3′ and 5′ co-terminal sgRNAs. Of note, the synthesis of sg mRNAs is not exclusive to the order *Nidovirales* but a discontinuous minus-strand synthesis strategy to produce a nested set of 3′ co-terminal sg mRNAs with a common 5′ leader in infected cells are unique features of the *coronaviruses* and *arteriviruses* [W. A. Miller and G. Koev.]. Of note, the produced genomic RNA represents a small fraction of the total vRNA [N. S. Ogando *et al.*].

The discontinuous minus-strand synthesis of a set of nested sg mRNAs happens during the synthesis of the negative-strand RNA, by an interruption mechanism of the RTC as it reads the TRS-B preceding each gene in the 3′ one-third of the viral genome [I. Sola, F. Almazan *et al.,* I. Sola, J. L. Moreno, *et al.*]. The synthesis of the negative-strand RNA stops and is re-initiated at the TRS-L of the genome sequence close from the 5′ end of the genome [H. Di *et al.*]. Therefore, the mechanism by which the leader sequence is added to the 5' end requires that the RTC switches template by a jumping mechanism. This interruption process involves the interaction between complementary TRSs of the nascent negative-strand RNA TRS-B and the positive-strand gRNA at the positive-sense TRS-L. The TRS-B site has a 7-8 bp conserved core sequence (CS) that facilitates RTC template switching as it hybridizes with a near complementary CS in the TRS-L [I. Sola, F. Almazan *et al.* I. Sola, J. L. Moreno, *et al.*]. Upon re-initiation of RNA synthesis at the TRS-L region, a negative-strand copy of the leader sequence is added to the nascent RNA to complete the synthesis of negative-strand sgRNAs. This means that all sg mRNAs as well as the genomic RNA share a common 5' sequence, named leader sequence [X. Zhang et al.]. This programmed template switching leads to the generation of sg mRNAs with identical 5' and 3' sequences, but alternative central regions corresponding to the beginning of each structural ORF [I. Sola *et al.* 2015, S. G. Sawicki *et al.*, Y. Yang *et al.*]. Of note, the existence of TRSs also raises the possibility that these sites are at the highest risk of recombining through TRS-B mediated template switching [Y. Yang]. The set of sg mRNAs is then translated to yield 29 identified different proteins [F. Wu *et al.*], although many papers have identified additional ORFs [D. Kim *et al..* Y. Finkel *et al.,* A. Vandelli *et al.*]. The translation of the linear single-stranded RNA conducts to the generation of the following proteome: 4 are structural proteins, S, N, M, and E; 16 proteins nsp: the first 11 are encoded in ORF1a whereas the last 5 are encoded in ORF1ab. In addition, 9 accessory proteins named ORF3a, ORF3b, ORF6, ORF7a, ORF7b, ORF8, ORF9b, ORF9c, and ORF10 have been identified [F. Wu *et al.*]. At the beginning of infection, there is the predominant expression of the nsp that result from ORF1a and ORF1ab, however, at 5 hpi, the proteins encoded by the 5′ last third are found in higher amounts, and the nucleoprotein is the protein found in higher levels [Y. Finkel *et al.*].

Viral assembly:

The final step of viral production requires virion assembly and this process is not well explored for SARS-CoV-2. For example, the role of the structural proteins of SARS-CoV-2 in virus assembly and budding in not known. In general, all beta-coronavirus structural proteins assemble at the endoplasmic reticulum (ER)-to-Golgi compartment [J. R. Cohen *et al.,* A. Perrier *et al.*] and viral assembly requires two steps: Genome packaging which is a process in which the SARS-CoV-2 gRNA must be coated by the viral protein nucleoprotein (N) protein, forming viral ribonucleoprotein (vRNPs) complexes, before being selectively packaged into progeny virions [P. V'Kovski *et al.*], a step in which vRNPs bud into the lumen of the ER and the ER-Golgi intermediate compartment (ERGIC) [N. S. Ogando *et al.*]. This results in viral particles enveloped with host membranes containing viral M, E, and S transmembrane structural proteins that need to be released from the cell.

SARS-CoV-2 gRNA packaging involves the N protein. The N protein of human coronaviruses is highly expressed in infected cells. It is considered a multifunctional protein, promoting efficient sub-genomic viral RNA transcription, viral replication, virion assembly, and interacting with multiple host proteins [P. V'Kovski *et al.*, D. E. Gordon *et al.*, R. McBride, and M. van Zyl, B. C.]. In relation to transcription and replication, the N protein could provide a cooperative mechanism to increase protein and RNA concentrations at specific localizations S. Alberti, and S. Carra, S. F. Banani *et al.*], and this way organize viral transcription. Five studies have shown that N protein undergoes liquid-liquid phase separation (LLPS) *in vitro* [A. Savastano *et al.*, H. Chen *et al.*, C. Iserman *et al.*, T. M. Perdikari *et al.*, J. Cubuk *et al.*], dependent on its C-terminal domain (CTD) [H. Chen *et al.].* It has been hypothesised that N could be involved in replication close to the ER and in packaging of gRNA into vRNPs near the ERGIC where genome assembly is thought to take place [A. Savastano *et al.*], but so far this is still speculative. Phosphorylation of N could adjust the physical properties of condensates differentially in ways that could accommodate the two different functions of N: transcription and progeny genome assembly [A. Savastano *et al.*, C. Iserman *et al.,* C. R. Carlson *et al.*].

The ERGIC constitutes the main assembly site of coronaviruses [S. Klein *et al.,* E. J. Snijder *et al.*, L. Mendonca *et al.*] and budding events have been seen by EM studies. For SARS-CoV-2, virus-budding was mainly clustered in regions with a high vesicle density and close to ER- and Golgi-like membrane arrangements [S. Klein *et al.,* E. J. Snijder *et al.*, L. Mendonca *et al.*]. The ectodomain of S trimers were found facing the ERGIC lumen and not induce membrane curvature on its own, therefore proposing that vRNPs and spike trimers [S. Klein *et al.*].

Finally, it has been shown that SARS-CoV-2 virions de novo formed traffic to lysosomes for unconventional egress by Arl8b-dependent lysosomal exocytosis [S. Ghosh *et al.*]. This process results in lysosome deacidification, inactivation of lysosomal degradation enzymes, and disruption of antigen presentation [S. Ghosh *et al.*].

How it is Measured or Detected

Viral translation:

SARS-CoV-2 Nsp1 binds the ribosomal mRNA channel to inhibit translation [Schubert *et al.* 2020]

- Sucrose pelleting binding assay to verify Nsp1–40S complex formation
- In vivo translation assay
- Transient expression of FLAG-Nsp1 in HeLa cells and puromycin incorporation assay

SARS-CoV-2 disrupts splicing, translation, and protein trafficking [Banerjee *et al.* 2020]

- SARS-CoV-2 viral protein binding to RNA
- Interferon stimulation experiments
- Splicing assessment experiments
- IRF7-GFP splicing reporter, 5EU RNA labeling, capture of biotinylated 5EU labeled RNA

Membrane SUnSET assay for transport of plasma membrane proteins to the cell surface

Viral transcription:

The mRNA transcripts are detected by the real-time reverse transcription-PCR (RT-PCR) assay. Several methods targeting the mRNA transcripts have been developed, which includes the RT-PCR assays targeting RdRp/helicase (Hel), spike (S), and nucleocapsid (N) genes of SARS-CoV-2 [Chan *et al.*]. RT-PCR assays detecting SARS-CoV-2 RNA in saliva include quantitative RT-PCR (RT-qPCR), direct RT-qPCR, reverse transcription-loop-mediated isothermal amplification (RT-LAMP) [Nagura-Ikeda M, *et al.*]. The viral mRNAs are reverse-transcribed with RT, followed by the amplification by PCR.

Viral replication:

viral replication is measured by RT-qPCR in infected cells, formation of liquid organelles is assessed in vitro reconstitution systems and in infected cells. Labelling by radioactive nucleosides.

Viral production:

Plaque assays, infectivity assays, RT-qPCR to detect viral RNA in released virions, sequencing to detect mutations in the genome, electron microscopy.

References

1. D. Kim *et al.*, The Architecture of SARS-CoV-2 Transcriptome. *Cell* **181**, 914-921 e910 (2020).

2. E. J. Snijder *et al.*, Unique and Conserved Features of Genome and Proteome of SARS-coronavirus, an Early Split-off From the Coronavirus Group 2 Lineage. *Journal of Molecular Biology* **331**, 991-1004 (2003).

3. N. C. Huston *et al.*, Comprehensive in vivo secondary structure of the SARS-CoV-2 genome reveals novel regulatory motifs and mechanisms. *Mol Cell* **81**, 584-598 e585 (2021).

4. C. J. Budzilowicz, S. P. Wilczynski, S. R. Weiss, Three intergenic regions of coronavirus mouse hepatitis virus strain A59 genome RNA contain a common nucleotide sequence that is homologous to the 3' end of the viral mRNA leader sequence. *J Virol* **53**, 834-840 (1985).

5. H. Di, A. A. McIntyre, M. A. Brinton, New insights about the regulation of Nidovirus subgenomic mRNA synthesis. *Virology* **517**, 38-43 (2018).

6. M. D. Sacco *et al.*, Structure and inhibition of the SARS-CoV-2 main protease reveal strategy for developing dual inhibitors against M(pro) and cathepsin L. *Sci Adv* **6**, (2020).

7. S. Klein *et al.*, SARS-CoV-2 structure and replication characterized by in situ cryo-electron tomography. *BioRxiv*, (2020).

8. E. J. Snijder *et al.*, A unifying structural and functional model of the coronavirus replication organelle: Tracking down RNA synthesis. *PLoS Biol* **18**, e3000715 (2020).

9. P. V'Kovski, A. Kratzel, S. Steiner, H. Stalder, V. Thiel, Coronavirus biology and replication: implications for SARS-CoV-2. *Nat Rev Microbiol*, (2020).

10. P. Liu, J. Leibowitz, in *Molecular Biology of the SARS-Coronavirus*. (2010), chap. Chapter 4, pp. 47-61.

11. V. B. O'Leary, O. J. Dolly, C. Hoschl, M. Cerna, S. V. Ovsepian, Unpacking Pandora From Its Box: Deciphering the Molecular Basis of the SARS-CoV-2 Coronavirus. *Int J Mol Sci* **22**, (2020).

12. Y. Finkel *et al.*, The coding capacity of SARS-CoV-2. *Nature* **589**, 125-130 (2021).

13. H. A. Hussein, R. Y. A. Hassan, M. Chino, F. Febbraio, Point-of-Care Diagnostics of COVID-19: From Current Work to Future Perspectives. *Sensors (Basel)* **20**, (2020).

14. M. Thoms *et al.*, Structural basis for translational shutdown and immune evasion by the Nsp1 protein of SARS-CoV-2. *Science* **369**, 1249-1255 (2020).

15. A. K. Banerjee *et al.*, SARS-CoV-2 Disrupts Splicing, Translation, and Protein Trafficking to Suppress Host Defenses. *Cell* **183**, 1325-1339 e1321 (2020).

16. H. Xia *et al.*, Evasion of Type I Interferon by SARS-CoV-2. *Cell Rep* **33**, 108234 (2020).

17. P. Ahlquist, RNA-dependent RNA polymerases, viruses, and RNA silencing. *Science* **296**, 1270-1273 (2002).

18. M. Schwartz *et al.*, A Positive-Strand RNA Virus Replication Complex Parallels Form and Function of Retrovirus Capsids. *Molecular Cell* **9**, 505-514 (2002).

19. W. A. Miller, G. Koev, Synthesis of subgenomic RNAs by positive-strand RNA viruses. *Virology* **273**, 1-8 (2000).

20. N. S. Ogando *et al.*, SARS-coronavirus-2 replication in Vero E6 cells: replication kinetics, rapid adaptation and cytopathology. *J Gen Virol* **101**, 925-940 (2020).

21. I. Sola, F. Almazan, S. Zuniga, L. Enjuanes, Continuous and Discontinuous RNA Synthesis in Coronaviruses. *Annu Rev Virol* **2**, 265-288 (2015).

22. I. Sola, J. L. Moreno, S. Zuniga, S. Alonso, L. Enjuanes, Role of nucleotides immediately flanking the transcription-regulating sequence core in coronavirus subgenomic mRNA synthesis. *J Virol* **79**, 2506-2516 (2005).

23. X. Zhang, C. L. Liao, M. M. Lai, Coronavirus leader RNA regulates and initiates subgenomic mRNA transcription both in trans and in cis. *J Virol* **68**, 4738-4746 (1994).

24. S. G. Sawicki, D. L. Sawicki, S. G. Siddell, A contemporary view of coronavirus transcription. *J Virol* **81**, 20-29 (2007).

25. Y. Yang, W. Yan, B. Hall, X. Jiang, Characterizing transcriptional regulatory sequences in coronaviruses and their role in recombination. *bioRxiv*, (2020).

26. F. Wu *et al.*, A new coronavirus associated with human respiratory disease in China. *Nature* **579**, 265-269 (2020).

27. A. Vandelli *et al.*, Structural analysis of SARS-CoV-2 genome and predictions of the human interactome. *Nucleic Acids Res* **48**, 11270-11283 (2020).

28. J. R. Cohen, L. D. Lin, C. E. Machamer, Identification of a Golgi complex-targeting signal in the cytoplasmic tail of the severe acute respiratory syndrome coronavirus envelope protein. *J Virol* **85**, 5794-5803 (2011).

29. A. Perrier *et al.*, The C-terminal domain of the MERS coronavirus M protein contains a trans-Golgi network localization signal. *J Biol Chem* **294**, 14406-14421 (2019).

30. D. E. Gordon *et al.*, A SARS-CoV-2 protein interaction map reveals targets for drug repurposing. *Nature* **583**, 459-468 (2020).

31. R. McBride, M. van Zyl, B. C. Fielding, The coronavirus nucleocapsid is a multifunctional protein. *Viruses* **6**, 2991-3018 (2014).

32. S. Alberti, S. Carra, Quality Control of Membraneless Organelles. *Journal of Molecular Biology* **430**, 4711-4729 (2018).

33. S. F. Banani, H. O. Lee, A. A. Hyman, M. K. Rosen, Biomolecular condensates: organizers of cellular biochemistry. *Nature Reviews Molecular Cell Biology* **18**, 285-298 (2017).

34. A. Savastano, A. I. de Opakua, M. Rankovic, M. Zweckstetter, Nucleocapsid protein of SARS-CoV-2 phase separates into RNA-rich polymerase-containing condensates. (2020).

35. H. Chen *et al.*, Liquid-liquid phase separation by SARS-CoV-2 nucleocapsid protein and RNA. *Cell Res*, (2020).

36. C. Iserman *et al.*, Specific viral RNA drives the SARS CoV-2 nucleocapsid to phase separate. *bioRxiv*, (2020).

37. T. M. Perdikari *et al.*, SARS-CoV-2 nucleocapsid protein undergoes liquid-liquid phase separation stimulated by RNA and partitions into phases of human ribonucleoproteins. *bioRxiv*, (2020).

38. J. Cubuk *et al.*, The SARS-CoV-2 nucleocapsid protein is dynamic, disordered, and phase separates with RNA. *bioRxiv*, (2020).

39. C. Iserman *et al.* (Cold Spring Harbor Laboratory, 2020).

40. C. R. Carlson *et al.*, Phosphoregulation of phase separation by the SARS-CoV-2 N protein suggests abiophysical basis for its dual functions. *Molecular Cell*, (2020).

41. L. Mendonca *et al.*, SARS-CoV-2 Assembly and Egress Pathway Revealed by Correlative Multi-modal Multi-scale Cryo-imaging. *bioRxiv*, (2020).

42. S. Ghosh *et al.*, beta-Coronaviruses Use Lysosomes for Egress Instead of the Biosynthetic Secretory Pathway. *Cell* **183**, 1520-1535 e1514 (2020).

43. Schubert, K., Karousis, E.D., Jomaa, A. *et al.* SARS-CoV-2 Nsp1 binds the ribosomal mRNA channel to inhibit translation. *Nat Struct Mol Biol* **27,** 959–966 (2020).

44. Chan, Jasper Fuk-Woo et al. Improved Molecular Diagnosis of COVID-19 by the Novel, Highly Sensitive and Specific COVID-19-RdRp/Hel Real-Time Reverse Transcription-PCR Assay Validated *In Vitro* and with Clinical Specimens. J Clin Microbiol. 2020:58(5)e00310-20. doi:10.1128/JCM.00310-20

45. Nagura-Ikeda M, Imai K, Tabata S, et al. Clinical Evaluation of Self-Collected Saliva by Quantitative Reverse Transcription-PCR (RT-qPCR), Direct RT-qPCR, Reverse Transcription-Loop-Mediated Isothermal Amplification, and a Rapid Antigen Test To Diagnose COVID-19. J Clin Microbiol. 2020;58(9):e01438-20. doi:10.1128/JCM.01438-20

46. Conceicao C, Thakur N, Human S, Kelly JT, Logan L, Bialy D, et al. (2020) The SARS-CoV-2 Spike protein has a broad tropism for mammalian ACE2 proteins. PLoS Biol 18(12): e3001016. https://doi.org/10.1371/journal.pbio.3001016

47. Damas J, Hughes GM, Keough KC, Painter CA, Persky NS, Corbo M, Hiller M, Koepfli KP, Pfenning AR, Zhao H, Genereux DP, Swofford R, Pollard KS, Ryder OA, Nweeia MT, Lindblad-Toh K, Teeling EC, Karlsson EK, Lewin HA. Broad host range of SARS-CoV-2 predicted by comparative and structural analysis of ACE2 in vertebrates. Proc Natl Acad Sci U S A. 2020 Sep 8;117(36):22311-22322. doi: 10.1073/pnas.2010146117. Epub 2020 Aug 21. PMID: 32826334; PMCID: PMC7486773.

List of Key Events in the AOP

Event: 1869: Oxidative stress response

Short Name: Response to ROS

Key Event Component

Process	Object	Action
cellular response to oxidative stress	reactive oxygen species	increased
response to reactive oxygen species	reactive oxygen species	increased

AOPs Including This Key Event

AOP ID and Name	Event Type
Aop:379 - Increased susceptibility to viral entry and coronavirus production leading to thrombosis and disseminated intravascular coagulation	KeyEvent

Stressors

Name
Stressor:624 SARS-CoV-2

Biological Context

Level of Biological Organization

Cellular

Cell term

Cell term

cell

Organ term

Organ term

organ

Domain of Applicability

Taxonomic Applicability

Term	Scientific Term	Evidence	Links
Homo sapiens	Homo sapiens	High	NCBI

Life Stage Applicability

Life Stage	Evidence
All life stages	High

Sex Applicability

Sex	Evidence
Unspecific	High

Response to ROS occurs in many cell types and tissues in all life stages and the broad range of mammals.

Key Event Description

Oxidative stress is caused by an imbalance between the production of reactive oxygen and the detoxification of reactive intermediates. Reactive intermediates such as peroxides and free radicals can be very damaging to many parts of cells such as proteins, lipids and DNA. Severe oxidative stress can trigger apoptosis and necrosis. [Ref. IPA, NRF2-mediated Oxidative Stress Response, version60467501, release date: 2020-11-19]

The cellular defence response to oxidative stress includes induction of detoxifying enzymes and antioxidant enzymes. Nuclear factor-erythroid 2-related factor 2 (Nrf2) binds to the antioxidant response elements (ARE) within the promoter of these enzymes and activates their transcription. Inactive Nrf2 is retained in the cytoplasm by association with an actin-binding protein Keap1. Upon exposure of cells to oxidative stress, Nrf2 is phosphorylated in response to the protein kinase C, phosphatidylinositol 3-kinase and MAP kinase pathways. After phosphorylation, Nrf2 translocates to the nucleus, binds AREs and transactivates detoxifying enzymes and antioxidant enzymes, such as glutathione S-transferase, cytochrome P450, NAD(P)H quinone oxidoreductase, heme oxygenase and superoxide dismutase. [Ref. IPA, NRF2-mediated Oxidative Stress Response, version60467501, release date: 2020-11-19]

Nrf2, a master regulator of oxidative stress through enhanced expression of anti-oxidant genes of glutathione and thioredoxin-antioxidant systems, has anti-inflammatory, anti-apoptotic, and anti-oxidant effects. Dimethyl fumarate (DMF), an activator of Nrf2, can decrease inflammation and reactive oxygen species (ROS) through the inhibition of NF-kappaB by inducing anti-oxidant enzymes [Hassan et al., MED ARCH. 2020 APR; 74(2): 134-138] [Timpani et al., Pharmaceuticals 2021, 14, 15.].

How it is Measured or Detected

Extracted from KE 1392 Oxidative Stress:

Oxidative Stress. Direct measurement of ROS is difficult because ROS are unstable. The presence of ROS can be assayed indirectly by measurement of cellular antioxidants, or by ROS-dependent cellular damage:

- Detection of ROS by chemiluminescence (https://www.sciencedirect.com/science/article/abs/pii/S0165993606001683) - Glutathione (GSH) depletion. GSH can be measured by assaying the ratio of reduced to oxidized glutathione (GSHGSSG) using a commercially available kit (e.g., https://www.abcam.com/gshgssg-ratio-detection-assay-kit-ii-fluorometric-green-ab205811.html). - TBARS. Oxidative damage to lipids can be measured by assaying for lipid peroxidation using TBARS (thiobarbituric acid reactive substances) using a commercially available kit. - 8-oxo-dG. Oxidative damage to nucleic acids can be assayed by measuring 8-oxo-dG adducts (for which there are a number of ELISA based

commercially available kits),or HPLC, described in Chepelev et al. [Chepelev, et al. 2015].

Molecular Biology: Nrf2. Nrf2′s transcriptional activity is controlled post-translationally by oxidation of Keap1. Assay for Nrf2 activity include: - Immunohistochemistry for increases in Nrf2 protein levels and translocation into the nucleus; - Western blot for increased Nrf2 protein levels; - Western blot of cytoplasmic and nuclear fractions to observe translocation of Nrf2 protein from the cytoplasm to the nucleus; - qPCR of Nrf2 target genes (e.g., Nqo1, Hmox-1, Gcl, Gst, Prx, TrxR, Srxn), or by commercially available pathway-based qPCR array (e.g., oxidative stress array from SABiosciences) - Whole transcriptome profiling by microarray or RNA-seq followed by pathway analysis (in IPA, DAVID, metacore, etc.) for enrichment of the Nrf2 oxidative stress response pathway (e.g., Jackson et al. 2014).

Extracted from KE 1753 Chronic reactive oxygen species for ROS detection:

ROS in blood can be detected using superparamagnetic iron oxide nanoparticles (SPION)-based biosensor (Lee et al., 2020).

ROS can be detected by fluorescent probes such as *p*-methoxy-phenol derivative (Ashoka et al., 2020).

References

1. Hassan SM, Jawad MJ, Ahjel SW, Singh RB, Singh J, Awad SM, Hadi NR. The Nrf2 Activator (DMF) and Covid-19: Is there a Possible Role? *Med Arch.* 2020 Apr;74(2):134-138. doi: 10.5455/medarh.2020.74.134-138. PMID: 32577056; PMCID: PMC7296400.

2. Timpani CA, Rybalka E. Calming the (Cytokine) Storm: Dimethyl Fumarate as a Therapeutic Candidate for COVID-19. *Pharmaceuticals*. 2021; 14(1):15. https://doi.org/10.3390/ph14010015

3. Chepelev, N.L.; Kennedy, D.A.; Gagné, R.; White, T.; Long, A.S.; Yauk, C.L., White, P.A. HPLC Measurement of the DNA Oxidation Biomarker, 8-oxo-7,8-dihydro-2'-deoxyguanosine, in Cultured Cells and Animal Tissues. *J Vis Exp* **2015**, e52697-e52697 [PMID: 26273842 DOI: 10.3791/52697]

4. Jackson, A.F.; Williams, A.; Recio, L.; Waters, M.D.; Lambert, I.B., Yauk, C.L. Case study on the utility of hepatic global gene expression profiling in the risk assessment of the carcinogen furan. *Toxicol Appl Pharmacol* **2014**, *274*, 63-77 [PMID: 24183702 DOI: 10.1016/j.taap.2013.10.019]

5. Lee, D. Y., Kang, S., Lee, Y., Kim, J. Y., Yoo, D., Jung, W., . . . Jon, S. (2020). PEGylated Bilirubin-coated Iron Oxide Nanoparticles as a Biosensor for Magnetic Relaxation Switching-based ROS Detection in Whole Blood. Theranostics, 10(5), 1997-2007. doi:10.7150/thno.39662

6. Ashoka, A. H., Ali, F., Tiwari, R., Kumari, R., Pramanik, S. K., & Das, A. (2020). Recent Advances in Fluorescent Probes for Detection of HOCl and HNO. *ACS omega, 5*(4), 1730-1742. doi:10.1021/acsomega.9b03420

Event: 1845: Coagulation

Short Name: Coagulation

AOPs Including This Key Event

AOP ID and Name	Event Type
Aop:379 - Increased susceptibility to viral entry and coronavirus production leading to thrombosis and disseminated intravascular coagulation	KeyEvent

Stressors

Name
Sars-CoV-2

Biological Context

Level of Biological Organization

Cellular

Cell term

Cell term

blood cell

Organ term

Organ term
blood plasma

Domain of Applicability

Taxonomic Applicability

Term	Scientific Term	Evidence	Links
Homo sapiens	Homo sapiens	Moderate	NCBI

Life Stage Applicability

Life Stage	Evidence
All life stages	Moderate

Sex Applicability

Sex	Evidence
Unspecific	Moderate

Homo sapiens

Key Event Description

Coagulation is a process that responds to injury by the rapid formation of a clot. Activation of coagulation factor proteins are involved in coagulation. In the extrinsic pathway, platelets, upon the contact with collagen in the injured blood vessel wall, release thromboxane A2 (TXA2) and adenosine 2 phosphates (ADP), leading to the clot formation. Extravascular tissue factor (TF) binds to plasma factor VIIa (FVIIa) and promotes the activation of FXa. Activated FXa assembles with cofactors FVa and FVIIIa on the surface of aggregated platelets, which lead to generation of thrombin (FIIa). Thrombin catalyzes the production of fibrin (FG) which creates a clot.
The binding of prekallikrein and high-molecular weight kininogen activate FXIIa in the intrinsic pathway.
Many regulators are involved in coagulation system. Plasmin is one of the modulators required for dissolution of the fibrin clot. Plasmin is activated by tissue plasminogen activator (tPA) and urokinase plasminogen activation (uPA). SERPINs inhibit thrombin, plasmin and tPA. For example, SERPINE1 or plasminogen activator inhibitor-1 (PAI-1) inhibits tPA/uPA and results in hypofibrinolysis [Bernard I,et al. Viruses. 2021; 13(1):29.]. In addition, SERPING1 inhibits FXII, and thus down-regulation of SERPING1 lifts suppression of FXII of the intrinsic coagulation cascade [Garvin et al. eLife 2020;9:e59177]. Protein C, protein S and thrombomodulin degrade FVa and FVIIIa. [Ref. IPA, Coagulation System, version60467501, release date: 2020-11-19]

How it is Measured or Detected

Coagulation and inflammatory parameters are measured in COVID-19 patients [Di Nisio et al. 2021]. Coagulation parameters include platelet count, prothrombin time, activated partial thromboplastin time, D-dimer, fibrinogen, antithrombin III [Di Nisio et al. 2021]. These parameters are measured in the blood.

In vitro systems

Whole human blood model for testing the activation of coagulation and complement system, as well as clot formation [Ekstrand-Hammarström, B. et al. Biomaterials 2015, 51, 58-68, Ekdahl, K.N., et al. Nanomedicine: Nanotechnology, Biology and Medicine 2018, 14, 735-744, Ekdahl, K.N., et al. Science and Technology of Advanced Materials, 20:1, 688-698,]

References

1. Bernard I, Limonta D, Mahal LK, Hobman TC. Endothelium Infection and Dysregulation by SARS-CoV-2: Evidence and Caveats in COVID-19. *Viruses*. 2021; 13(1):29. DOI: https://doi.org/10.3390/v13010029
2. Garvin et al. A mechanistic model and therapeutic interventions for COVID-19 involving a RAS-mediated bradykinin storm. *eLife* 2020;9:e59177. DOI: https://doi.org/10.7554/eLife.59177
3. Di Nisio, Marcello et al. Interleukin-6 receptor blockade with subcutaneous tocilizumab improves coagulation activity in patients with COVID-19 European Journal of Internal Medicine, Volume 83, 34 - 38 DOI: https://doi.org/10.1016/j.ejim.2020.10.020
4. Ekstrand-Hammarström, B.; Hong, J.; Davoodpour, P.; Sandholm, K.; Ekdahl, K.N.; Bucht, A., Nilsson, B. TiO2 nanoparticles tested in a novel screening whole human blood model of toxicity trigger adverse activation of the kallikrein system at low concentrations. Biomaterials 2015, 51, 58-68 DOI:https://doi.org/10.1016/j.biomaterials.2015.01.031
5. Ekdahl, K.N.; Davoodpour, P.; Ekstrand-Hammarström, B.; Fromell, K.; Hamad, O.A.; Hong, J.; Bucht, A.; Mohlin, C.; Seisenbaeva, G.A.; Kessler, V.G., Nilsson, B. Contact (kallikrein/kinin) system activation in whole human blood induced by low concentrations of α-Fe2O3 nanoparticles. Nanomedicine: Nanotechnology, Biology and Medicine 2018, 14, 735-744 [DOI: https://doi.org/10.1016/j.nano.2017.12.008]

6. Kristina N Ekdahl, Karin Fromell, Camilla Mohlin, Yuji Teramura & Bo Nilsson (2019) A human whole-blood model to study the activation of innate immunity system triggered by nanoparticles as a demonstrator for toxicity, Science and Technology of Advanced Materials, 20:1, 688-698, DOI: 10.1080/14686996.2019.1625721

List of Adverse Outcomes in this AOP

Event: 1846: Thrombosis and Disseminated Intravascular Coagulation

Short Name: Thrombosis and DIC

Key Event Component

Process	Object	Action
Venous thrombosis	platelet	increased

AOPs Including This Key Event

AOP ID and Name	Event Type
Aop:379 - Increased susceptibility to viral entry and coronavirus production leading to thrombosis and disseminated intravascular coagulation	AdverseOutcome

Stressors

Name
Sars-CoV-2

Biological Context

Level of Biological Organization
Organ

Organ term

Organ term
blood

Domain of Applicability

Taxonomic Applicability

Term	Scientific Term	Evidence	Links
Homo sapiens	Homo sapiens	Moderate	NCBI

Life Stage Applicability

Life Stage	Evidence
All life stages	Not Specified

Sex Applicability

Sex	Evidence
Unspecific	Not Specified

Homo sapiens

Key Event Description

Thrombosis is defined as the formation or presence of a thrombus. Clotting within a blood vessel may cause infarction of tissues

supplied by the vessel. Extreme aggravation of blood coagulation induces multiple thrombi in the microvasculature, which leads to consumption coagulopathy followed by disseminated intravascular coagulation (DIC).

DIC is a pathological syndrome resulting from the formation of thrombin, subsequent activation and consumption of coagulation proteins, and the production of fibrin thrombi. The initial pathologic events are thrombotic in nature resulting in thrombotic vascular occlusions. The initial clinical events are usually hemorrhagic resulting in oozing from mucosa and massive gastrointestinal blood loss. The occlusive events occur as a result of fibrin microthrombi or platelet microthrombi that obstruct the microcirculation of organs. This obstruction can result in organ hypoperfusion and ischemia, infarction, and necrosis. All organs are potentially vulnerable to the effects of thrombotic occlusions.

The renal effects of DIC are multifactorial and may be associated with hypovolemia or hypotension. If the hypotension is not corrected it may lead to renal failure due to acute tubular necrosis. Fibrin thrombi may also block glomerular capillaries causing ischemic, renal cortical necrosis (Colman, 1984).

The cerebral effects of DIC often result in nonspecific changes such as altered state of consciousness, convulsions, and coma. Major vascular occlusions, subarachnoid hemorrhage, multiple cortical and brain stem hemorrhages may occur following microvascular occlusions (Schwartzman RJ, 1982).

The pulmonary effects of DIC may be caused by interstitial hemorrhage resulting in a clinical effect resembling acute respiratory distress syndrome (Schwartzman RJ,1973; Shahl RL, 1984).

How it is Measured or Detected

Clinical laboratory tests are used to diagnose DIC.

Prothrombin time (**PT**) is a blood test that measures how long it takes blood to clot. PT measures the time required for fibrin clot formation after the addition of tissue thromboplastin and calcium. The average time range for blood to clot is about 10 to 13 seconds.

Activated partial prothrombin time (APTT). Platelet poor plasma [PPP] is incubated at 37°C then phospholipid (cephalin) and a contact activator (e.g. Kaolin, micronized silica, or ellagic acid) are added. This leads to the conversion of Factor XI [FXI] to FXIa. The remainder of the pathway is not activated as no calcium is present. The addition of calcium (pre-warmed to 37°C) initiates clotting. The APTT is the time taken from the addition of calcium to the formation of a fibrin clot. The clotting time for the APTT lies between 27-35 seconds.

Decreased fibrinogen concentrations

Diluted plasma is clotted with a high concentration of Thrombin. The tested plasma is diluted (usually 1:10 but this may vary if the Fibrinogen concentration is very low or very high) to minimize the effect of 'inhibitory substances' within the plasma e.g. heparin, elevated levels of FDPs. The use of a high concentration of Thrombin (typically 100 U/ml) ensures that the clotting times are independent of Thrombin concentration over a wide range of Fibrinogen levels.

The test requires a reference plasma with a known Fibrinogen concentration and that has been calibrated against a known international reference standard. A calibration curve is constructed using this reference plasma by preparing a series of dilutions (1:5 –1:40) in the buffer to give a range of Fibrinogen concentrations. The clotting time of each of these dilutions is established (using duplicate samples) and the results (clotting time(s)/Fibrinogen concentration (g/L) are plotted on Log-Log graph paper. The 1:10 concentration is considered to be 100% i.e. normal. There should be a linear correlation between clotting times in the region of 10-50 sec.

The test platelet-poor diluted plasma (diluted 1:10 in buffer) is incubated at 37°C, Thrombin [~100 U/mL] added (all pre-warmed to 37°C). The time taken for the clot to form is compared to the calibration curve and the Fibrinogen concentration deduced. Test samples whose clotting times fall out with the linear part of the calibration curve should be re-tested using different dilutions.

Most laboratories use an automated method in which clot formation is deemed to have occurred when the optical density of the mixture has exceeded a certain threshold.

Platelet Measurements-

A platelet count is the number of platelets a person has per microliter. The ideal platelet range is 150,000 – 400,000 per microliter in most healthy people.

Fibrinolysis measurements-

- d-dimer concentration ALERE TRIAGE® D-DIMER TEST

D-Dimer can be measured by a fluorescence immunoassay. To determine cross-linked fibrin degradation products containing D-dimer in EDTA anticoagulated whole blood and plasma specimens. The test is used as an aid in the assessment and evaluation

of patients suspected of having disseminated intravascular coagulation or thromboembolic events including pulmonary embolism

Procedure:

Commercially available kits are available to measure d-dimer in whole blood or plasma. The kits contain all the reagents necessary for the quantification of cross-linked fibrin degradation products containing D-dimer in EDTA anticoagulated whole blood or plasma specimens.

Regulatory Significance of the AO

Thrombosis is one of the world's main concerns in terms of severe symptoms or adverse responses of the vaccine for COVID-19 which is caused by SARS-CoV-2. Excess thrombosis leads to DIC, which might be mortal. For safely developing the therapeutics and vaccines of COVID-19, it is regulatory significant to understand the cellular and molecular mechanisms in the pathogenesis of coronaviral infection, which may include thrombosis and DIC, AO1846.

References

Hemostasis and Thrombosis Basic Principles and Clinical Practices Robert W Colman, Jack Hirsh, Victor J. Marder, Edwin W. Salzman (ed) Philadelphia, 1994.

Schwartzman RJ, Hill JB: Neurologic complications of DIC. Neurology 32:791, 1982

Robboy SJ, Minna JD, Colman RW et.al. Pulmonary hemorrhage syndrome as a manifestation of DIC: Analysis of 10 cases. Chest 63:718, 1973.

Stahl RL, Javid JP, Lackner H: Unrecognized pulmonary embolism presenting as DIC. SM J Med 76:772, 1984.

Appendix 2

List of Key Event Relationships in the AOP

List of Adjacent Key Event Relationships

Relationship: 2310: Increased susceptibility to viral entry leads to Increased SARS-CoV-2 production

AOPs Referencing Relationship

AOP Name	Adjacency	Weight of Evidence	Quantitative Understanding
Increased susceptibility to viral entry and coronavirus production leading to thrombosis and disseminated intravascular coagulation	adjacent	High	Moderate
Binding of viral S-glycoprotein to ACE2 receptor leading to acute respiratory distress associated mortality	adjacent	High	High

Relationship: 2358: Increased SARS-CoV-2 production leads to Response to ROS

AOPs Referencing Relationship

AOP Name	Adjacency	Weight of Evidence	Quantitative Understanding
Increased susceptibility to viral entry and coronavirus production leading to thrombosis and disseminated intravascular coagulation	adjacent	Moderate	Not Specified

Relationship: 2359: Response to ROS leads to Coagulation

AOPs Referencing Relationship

AOP Name	Adjacency	Weight of Evidence	Quantitative Understanding
Increased susceptibility to viral entry and coronavirus production leading to			

AOP Name	Adjacency	Weight of Evidence	Quantitative Understanding
thrombosis and disseminated intravascular coagulation	adjacent	Moderate	Not Specified

Relationship: 2360: Coagulation leads to Response to ROS

AOPs Referencing Relationship

AOP Name	Adjacency	Weight of Evidence	Quantitative Understanding
Increased susceptibility to viral entry and coronavirus production leading to thrombosis and disseminated intravascular coagulation	adjacent	Moderate	Not Specified

Relationship: 2290: Coagulation leads to Thrombosis and DIC

AOPs Referencing Relationship

AOP Name	Adjacency	Weight of Evidence	Quantitative Understanding
Increased susceptibility to viral entry and coronavirus production leading to thrombosis and disseminated intravascular coagulation	adjacent	High	

Evidence Supporting Applicability of this Relationship

Taxonomic Applicability

Term	Scientific Term	Evidence	Links
Homo sapiens	Homo sapiens	High	NCBI

Life Stage Applicability

Life Stage	Evidence
All life stages	High

Sex Applicability

Sex	Evidence
Unspecific	High

Key Event Relationship Description

Many regulators are involved in coagulation system. Plasmin is one of the modulators required for dissolution of the fibrin clot. Plasmin is activated by tissue plasminogen activator (tPA) and urokinase plasminogen activation (uPA). SERPINs inhibit thrombin, plasmin and tPA. For example, SERPINE1 or plasminogen activator inhibitor-1 (PAI-1) inhibits tPA/uPA and results in hypofibrinolysis [Bernard I,et al. Viruses. 2021; 13(1):29.]. In addition, SERPING1 inhibits FXII, and thus down-regulation of SERPING1 lifts suppression of FXII of the intrinsic coagulation cascade [Garvin et al. eLife 2020;9:e59177]. Protein C, protein S and thrombomodulin degrade FVa and FVIIIa. [Ref. IPA, Coagulation System, version60467501, release date: 2020-11-19]

Quantitative Understanding of the Linkage

Known Feedforward/Feedback loops influencing this KER

Decreased fibrinolysis is involved in coagulation system. Coagulopathy may also be involved in this KER. [Mast AE et al, Garvin MR et al.]

References

1. Bernard I, Limonta D, Mahal LK, Hobman TC. Endothelium Infection and Dysregulation by SARS-CoV-2: Evidence and Caveats in COVID-19. *Viruses*. 2021; 13(1):29. DOI: https://doi.org/10.3390/v13010029
2. Garvin et al. A mechanistic model and therapeutic interventions for COVID-19 involving a RAS-mediated bradykinin storm. *eLife* 2020;9:e59177. DOI: https://doi.org/10.7554/eLife.59177
3. Mast AE, Wolberg AS, Gailani D, Garvin MR, Alvarez C, Miller JI, Aronow B, Jacobson D (2021) SARS-CoV-2 suppresses anticoagulant and fibrinolytic gene expression in the lung. eLife 10:e64330. doi:10.7554/eLife.64330

4. Garvin MR, Alvarez C, Miller JI, Prates ET, Walker AM, Amos BK, Mast AE, Justice A, Aronow B, Jacobson D (2020) A mechanistic model and therapeutic interventions for COVID-19 involving a RAS-mediated bradykinin storm. eLife 9:e59177. doi:10.7554/eLife.59177